Microphysical simulations of mesospheric CO_2 ice clouds and comparison to observations

C. Listowski, LATMOS, UVSQ, (constantino.listowski@latmos.ipsl.fr)**, A. Määttänen,** LATMOS, UVSQ, CNRS **, F. Montmessin,** LATMOS, UVSQ, CNRS**, A. Spiga,** LMD, UPMC, **F. Lefèvre,** LATMOS, UPMC

Introduction:

Since the first unambiguous spectral detection of a CO_2 ice cloud [15], how the main atmospheric component of the martian atmosphere (~95%) condenses to form CO_2 ice clouds in the mesosphere has not been fully addressed theoretically. Mesospheric daytime clouds (reff~1 μm, τ~0.1) [15,16,22] and nighttime clouds (reff~0.1 μm, τ~0.01) [14] remain to be explained by modeling. [4] has been the only attempt to simulate daytime mesospheric clouds with a Martian GCM. Crystal sizes close although bigger than observed values for daytime clouds were obtained, but spatial and temporal coverage were not in agreement with observations [8].

A recent modeling study shows that thermal tides are a prerequisite for CO_2 clouds formation and that minimum temperatures predicted in the mesosphere by the LMD-GCM [6,8] are correlated with the observations of mesospheric clouds [9]. However smaller scale processes are needed to attain CO_2 supersaturation in the mesosphere [9]. Furthermore, modeling has shown that locations where gravity waves are theoretically able to propagate up to the mesosphere are correlated with locations where CO_2 ice clouds have been observed [18]. We thus simulate for the first time wave-induced mesospheric CO_2 ice clouds with a 1D-model, using temperature profiles accounting for large-scale (thermal tides) and meso-scale (gravity waves) perturbations. Doing so, we follow for the first time a scenario already suggested by [3]: "*As a result CO_2 ice clouds should form within the temperature minima of tidal and gravity waves in the Mars mesosphere, and be fairly common phenomena at low-to-mid latitudes during day and night times*."

We will present results obtained with the 1D-simulations of mesospheric CO_2 ice clouds within cold pockets created by gravity waves, and compare them to observations. Simple dust scenarios are prescribed to account for condensation nuclei, necessary to explain measured opacities.

Model and Method:

Mircophysical processes. A 1D microphysical model previously used to simulate water ice clouds on Mars [12] was adapted to the mixture 95% CO_2/ 5% N_2, following previous modeling studies of CO_2 polar ice clouds [4,23]. The model goes up to 120 km altitude and the radius grid extends from 1 nm to 100 μm. We use heterogeneous nucleation, as it is the most likely process to trigger crystal growth in the martian mesosphere [15]. Vertical transport is implemented according to [19]. Sedimentation is corrected to account for vertical mixing parameterized by a diffusion coefficient k_d. Growth rate of crystals is derived using the model of [11] adapted to the condensation of a near-pure vapor in a rarefied atmosphere, within highly supersaturated atmospheric layers (S>>1) [e.g. 7].

Trace-gas approximation. Pressure levels of the model are fixed. They remain fixed during cloud simulation despite CO_2 condensation. If m_a is the mass of an atmospheric layer $dm_a/m_a \leq 1\%$ as long as $dq_{ice} \leq 3.10^{-4}$, where dq_{ice} is the variation of the mass mixing ratio of ice. We show that despite this limitation, mesospheric clouds in agreement with observations can be simulated.

Temperature profiles. We use temperature profiles from meso-scale modeling obtained as explained in [12]. Large-scale temperature profiles from the LMD-GCM [6] extending to the exosphere [8] are used to constrain the meso-scale domain where gravity waves are simulated. Discrepancies of large-scale temperature profiles between LMD-GCM outputs and measurements have been observed [7]. Thus it is necessary to shift the modeled temperature profile by a constant value to investigate a broad range of plausible mesospheric supersaturations. The gravity wave amplitude remains unchanged by this shift. Various supersaturated layers (cold pockets) are simulated, allowing for CO_2 condensation at high mesospheric altitudes (here, ≥70 km).

Dust profile. Equilibrium dust profiles are a result of sedimentation and vertical mixing processes. We use profiles which bracket average dust conditions as given by the Mars Climate Database [12], and are typical of epochs of CO_2 cloud formation.

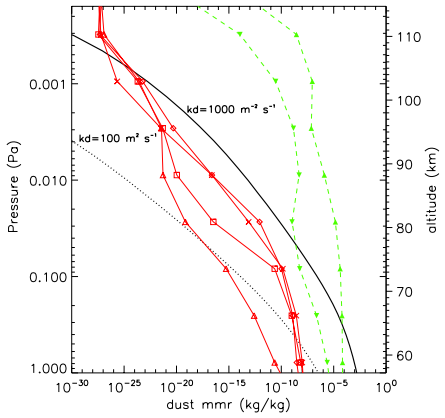

Figure 1 Vertical profile of mass mixing ratio of dust from our model (black) compared to average dust content during CO2 cloud formation epochs (red) from [12], and compared to dust storm conditions (green) from [12].

Results:

Crystal Sizes. Typical size of 1 µm for daytime clouds are obtained with a gravity wave causing a maximum S around 60 between 70 and 80 km altitude (Fig. 2). Typical sizes of 100 nm are simulated for nighttime clouds at around 90 km with a gravity wave causing S of a few hundreds (Fig. 3). Both cases are also in agreement with measurements of saturation ratios at the respective altitudes.

More generally, we show that the altitude of crystal formation is mainly responsible for their difference in sizes between daytime and nighttime clouds due to distinct condensation efficiencies at different atmospheric pressures. The supersaturation amplitude has a secondary influence on the crystal size compared to the altitude of cloud formation.

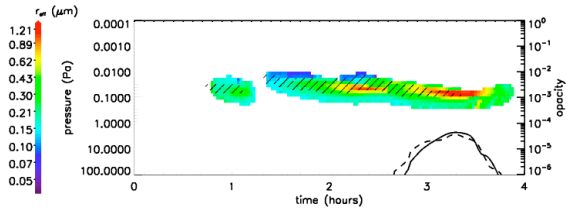

Figure 2 Effective radius of crystals (colorscale) versus elapsed time, in a daytime cloud formed in a cold pocket (shaded area). Y-axis is pressure (left) and opacity at 1 µm.

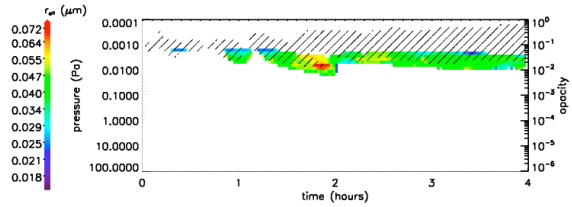

Figure 3 Effective radius of crystals (colorscale) versus elapsed time, in a nighttime cloud formed in a cold pocket (shaded area). Y-axis is pressure (left) and null opacity at 200 nm.

Opacities.

Opacities are far below observed values, by several orders of magnitude, suggesting a lack of condensation nuclei (CN). Dust profiles closer to dust content typical of dust storms and/or meteoritic supply can help to achieve the larger opacities observed (Fig. 4 and 5). Meteoritic input is prescribed in agreement with published estimations for Mars [5,17] and CN sizes are ≤10 nm as expected from terrestrial meteoroid ablation simulations [2,10]

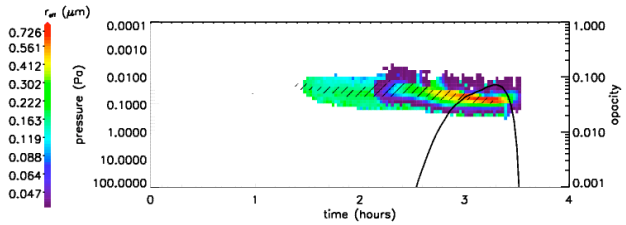

Figure 4 Effective radius of crystals (colorscale) versus elapsed time, in a daytime cloud formed in a cold pocket (shaded area) with meteoritic flux of 10 nm particles. Y-axis is pressure (left) and opacity at 1 µm (right).

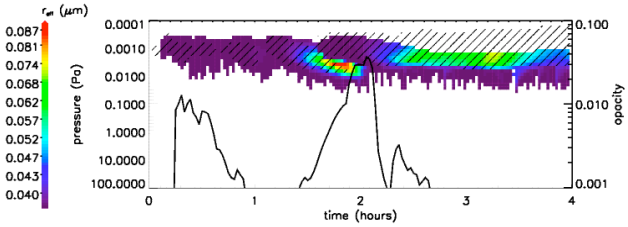

Figure 5 Effective radius of crystals (colorscale) versus elapsed time, in a nighttime cloud formed in a cold pocket (shaded area) with meteoritic flux of 10 nm particles. Y-axis is pressure (left) and opacity at 200 nm (right).

Discussion :

Supply of CN. Dust storm alone cannot explain the formation of optically thick CO_2 ice clouds along the whole period of observation (Ls=0°-140°), due to short residence time of particles. Thus, an exogenic supply of condensation nuclei seems necessary to account for the observation of thick clouds until Ls=140°. Meteoritic particles are a good candidate for condensation nuclei. Indeed, ablation of meteoroids in the atmosphere, responsible for the formation of nanometric particles, theoretically occurs in the altitude range [1] where CO_2 clouds form. In addition to that, electron layers of meteoritic origin have been observed in the altitude range 70–100 km [18] confirming the ablation altitude range.

Clouds and waves. The cloud evaporates fast after the cold pocket has vanished. This suggests a close link between the gravity wave passage and mesospheric cloud formation. The cloud lifetime is related to the cold pocket lifetime and it seems unlikely to observe a cloud in a sub-saturated area. However the four cases of nighttime CO_2 mesospheric clouds re-

ported by [14] show mostly clouds detected below the concomitant supersaturated layer. [14] explained this shift by the sedimentation of the cloud out of the cold pocket responsible of its formation, while [22] suggested a different composition for these clouds (H_2O). We rather explain this shift by the behavior of the cold pocket actually responsible of the cloud formation, which would have vanished, leaving the cloud in a sub-saturated air (Fig. 6). The clouds need to have been observed very soon after the cold pocket had vanished since the lifetime is of the order of ten minutes.

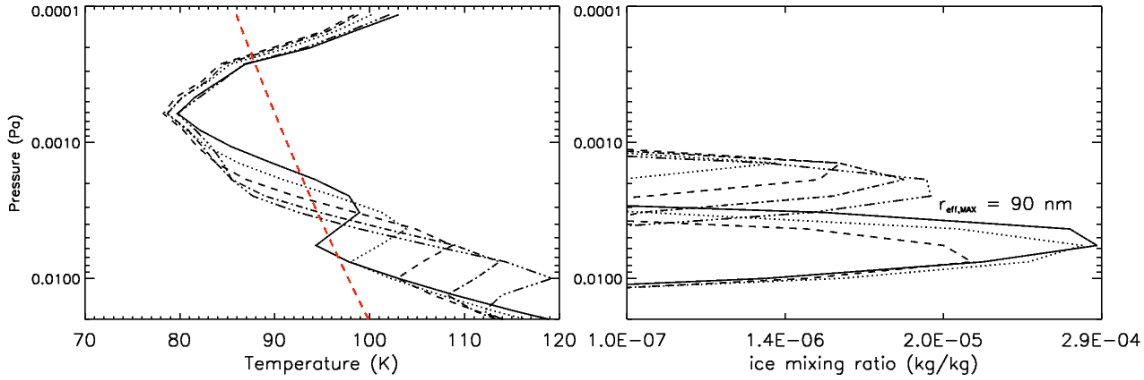

Figure 6 Selection of vertical profiles (plotted every 300 s.) of temperature (left) and ice mixing ratio (right) of the cloud presented in Figure 5. The dashed line on the left plot represents the CO2 condensation temperature. A shift between the main cold pocket and the main cloud is observed.

Conclusion :

We present the first time ever simulations of mesospheric clouds within cold pockets created by gravity waves. We are able to reproduce the observed effective sizes of CO_2 cloud crystals at the corresponding altitudes, but not the opacities, provided that we remain with average dust conditions. An additional supply of nuclei is needed to explain the measured opacities. A likely candidate would be the meteoric particles coming from meteoroid ablation in the mesosphere. Gravity waves causing saturation ratios in accordance with observations allow simulating clouds in agreement with day and night observations. Finally, the temporal/spatial behavior of the cold pocket determines the temporal/spatial behavior of the cloud.

References :

[1] Adolfson et al., 1996
[2] Bardeen et al., JGR-A,113,17202, 2008
[3] Clancy and Sandor, GRL,25(4), 489–492,1998
[4] Colaprete, et al. PSS, 56, 150C,2008
[5] Flynn an McKay, JGR,95, 14497–14509, 1990
[6] Forget et a., JGR,104,E10, 1999
[7] Forget et al., JGRE, 114,E01004,2009
[8] Gonzalez-Galindo et al, JGR, 114, E04001, 2009
[9] Gonzalez-Galindo et al, 216, 10–22, 2011
[10] Hunten et al., J. Atmos. Sci. 37, 1342., 1980
[11] Listowski et al., J*GR Planets, 118, 2013*
[12] Millour et al.in: EPSC Congress, p. 302, 2012
[13] Montmessin et al., JGR, 107, 2002
[14] Montmessin et al., Icarus, 183, 2006
[15] Montmessin et al., JGR, 112, E11S90, 2007
[16] Määttänen et al., Icarus, 209,452–469, 2010
[17] Nesvorny et al., ApJ, 713,816–836, 2010
[18] Patzöld et al., Science 310, 837–839, 2005
[19] Spiga, and Forget, JGR., 114, E02009, 2009
[20] Spiga et al., GRL, 39, L02201, 2012
[21] Toon et al., JGR, 1994, 11359—11380, 1989
[22] Vincendon et al., JGR,116, 2011
[23] Wood, 1999, PhD, UCLA, 1999